Experimental Observation and Spin Texture of Dirac Node Arcs in Tetradymite Topological Metals

J. Dai,[1,*,§] E. Frantzeskakis,[1,†] N. Aryal,[2,3,‖] K.-W. Chen,[2,3,¶] F. Fortuna,[1] J. E. Rault,[4] P. Le Fèvre,[4] L. Balicas,[2,3] K. Miyamoto,[5] T. Okuda,[5] E. Manousakis,[2,3,6] R. E. Baumbach,[2,3] and A. F. Santander-Syro[1,‡]

[1]*Université Paris-Saclay, CNRS, Institut des Sciences Moléculaires d'Orsay, 91405 Orsay, France*
[2]*National High Magnetic Field Laboratory, Florida State University, Tallahassee, Florida 32306, USA*
[3]*Department of Physics, Florida State University, Tallahassee, Florida 32306, USA*
[4]*Synchrotron SOLEIL, L'Orme des Merisiers, Saint-Aubin-BP48, 91192 Gif-sur-Yvette, France*
[5]*Hiroshima Synchrotron Radiation Center (HSRC), Hiroshima University, 2-313 Kagamiyama, Higashi-Hiroshima 739-0046, Japan*
[6]*Department of Physics, National and Kapodistrian University of Athens, Panepistimioupolis, Zografos, 157 84 Athens, Greece*

(Received 15 November 2020; revised 8 March 2021; accepted 15 April 2021; published 14 May 2021)

We report the observation of a nontrivial spin texture in Dirac node arcs, i.e., novel topological objects formed when Dirac cones of massless particles extend along an open one-dimensional line in momentum space. We find that such states are present in all the compounds of the tetradymite M_2Te_2X family (M = Ti, Zr, or Hf and X = P or As) regardless of the weak or strong character of the topological invariant. The Dirac node arcs in tetradymites are thus the simplest possible textbook example of a type-I Dirac system with a single spin-polarized node arc.

DOI: 10.1103/PhysRevLett.126.196407

During the last decade, various topological phases of matter such as the quantum spin Hall effect [1,2], topological insulators [3,4], topological superconductors [5], topological crystalline insulators [6], or Dirac and Weyl semimetals [7–10] have provoked an immense interest in the scientific community. Scientific excitement in topological matter stems from the matter's high potential in novel applications such as building blocks of quantum information in the form of Majorana zero modes [11,12], spin generators in spintronic circuits [13,14], and optoelectronic nanodevices [15].

Dirac cones, the simplest form of topological states, can have variable dimensionality in momentum space ranging from 1D to 3D, and they can display different topological characteristics that give rise to weak and strong topological states. Moreover, when the Dirac cone extends along an open 1D line in momentum space, the series of adjacent Dirac points form so-called "Dirac node arcs" [16,17]. Each variation in the dimensionality, topological characteristics, and *k*-space fingerprint of the Dirac point (i.e., a single node vs a 1D line or arc) defines a new class of topological matter: quantum spin Hall insulators for 1D states [2,18], strong or weak topological insulators for 2D states [19–21], Dirac and Weyl semimetals for 3D states [8–10,22], and nodal-line semimetals for Dirac nodal lines [23–25].

There is, however, a new family of topological metals that is predicted to combine many of the above special features. This is the tetradymite family M_2Te_2X (with M = Ti, Zr, or Hf and X = P or As) in which both strong and weak topological surface states have been theoretically predicted [26–29], interestingly accompanied by Dirac node arcs in one of its members [29]. In this work, we employ angle- and spin-resolved photoemission spectroscopy (ARPES and SARPES) to experimentally demonstrate the crucial but still missing evidence that such Dirac node arcs are *spin-polarized*, showing a nontrivial spin texture, and hence they meet all the essential requirement to be classified as *topological Dirac node arcs*. Moreover, our results prove that *all* compounds of the family share the exotic feature of a Dirac node arc. Compared to Dirac node arcs observed in topological line-node semimetals [17,30] or to multiple node arcs in type-I Dirac systems [16], the unique Dirac node arc in the tetradymite M_2Te_2X compounds is thus the simplest possible textbook example of a type-I Dirac system with a single spin-polarized node arc.

The ARPES experiments were performed at the CASSIOPEE beamline of Synchrotron SOLEIL (France), and the Spin-ARPES experiments were performed using the ESPRESSO machine at beamline 9B of the Hiroshima Synchrotron Radiation Center (HiSOR, Japan) [31]. Typical energy and angular resolutions were 15 meV and 0.25°. The single crystals of M_2Te_2X (M = Ti, Zr, or Hf and X = P or As) [26] were cleaved *in situ* at temperatures below 25 K and pressure in the range of 10^{-11} mbar and were kept at those conditions during the measurements. The Supplemental Material [32] provides complete technical details about the sample growth, crystal structure, and ARPES and Spin-ARPES measurements.

Figure 1(a) presents the experimental constant energy contours of Ti_2Te_2P at various binding energies. The Fermi surface consists of six petallike electron pockets centered at

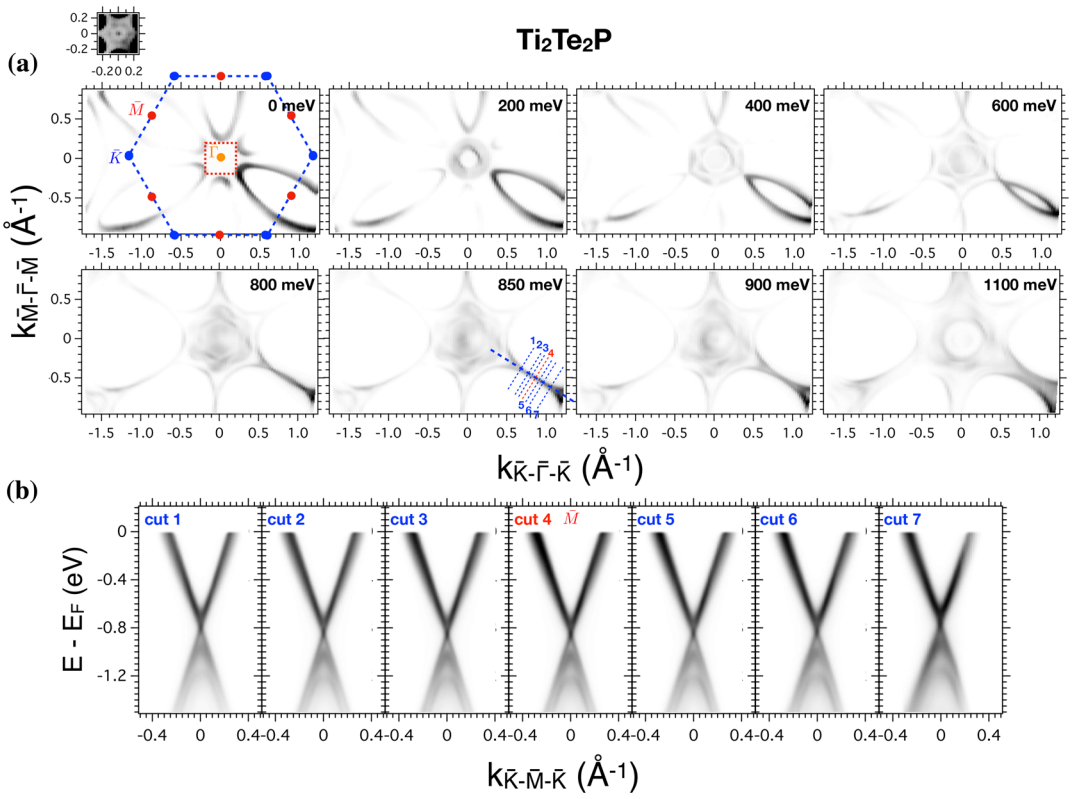

FIG. 1. (a) Constant energy maps at various binding energies. A linear feature appears at an approximate binding energy of 850 meV. The dashed blue hexagon marks the borders of the surface-projected Brillouin zone. The dashed red square indicates the area with saturated contrast shown in the inset above the top left panel. (b) Energy-momentum dispersion showing a persistent Dirac-like dispersion along various k paths marked by dashed lines in (a). All data were collected using photons of 50 eV and linear horizontal polarization. The temperature was 6 K.

the $\bar{\mathrm{M}}$ points of the surface Brillouin zone and a weaker hexagonal contour in the immediate vicinity of $\bar{\Gamma}$ [28], shown in the inset. The smallest pointlike contour at $\bar{\Gamma}$ is residual intensity coming from a holelike band whose maximum lies just below E_F for Ti_2Te_2P [28]. As the binding energy increases, the petallike contours evolve into linear features along the $\overline{\Gamma M}$ high symmetry lines. The energy-momentum dispersion along $\overline{\mathrm{KMK}}$ reveals a Dirac cone that is typical for all compounds of the tetradymite family M_2Te_2X. Our previous first-principles calculations [28] revealed the nontrivial origin of such Dirac-like states. The binding energy of the Dirac point for Ti_2Te_2P is 0.85 eV, that is, 200–300 meV lower than for other compounds of this family (see Fig. S2). Interestingly, as shown in panel (b) by the energy-momentum maps along the k paths parallel to $\overline{\mathrm{KMK}}$, this Dirac-like dispersion is present all along the linear features of the constant energy map, with the Dirac point shifting to slightly lower binding energies as one moves away from $\bar{\mathrm{M}}$ (see Fig. S3). These results are in agreement with a previous study on Hf_2Te_2P [29], and they present a first indication that these linear features may correspond to topologically nontrivial Dirac node arcs. The Supplemental Material [32] presents additional data and analyses for the linearly dispersing Dirac states in the vicinity of $\overline{M}$ along $\overline{\mathrm{KMK}}$, as well as for the Dirac node arcs, for Hf_2Te_2P, Zr_2Te_2P, Ti_2Te_2P, and Zr_2Te_2As.

Without any information on their spin texture, the linear features in the constant energy maps of the M_2Te_2X compounds (see Fig. S3), even if associated with a conelike dispersion, cannot be unambiguously assigned to topologically nontrivial Dirac node arcs. Thus, a direct measurement of their spin polarization is necessary to elucidate if they correspond to nontrivial states. As we will see next, our SARPES data on Ti_2Te_2P and Hf_2Te_2P reveal an appreciable spin polarization of the Dirac cones, both along $\overline{\mathrm{KMK}}$ and at parallel k paths. As a result, they establish the linear features of the constant energy maps as topologically nontrivial 1D Dirac node arcs.

Figure 2 presents spin-integrated and spin-resolved ARPES results acquired using the ESPRESSO setup at HiSOR [31] on Ti_2Te_2P [Figs. 2(a), (b)] and Hf_2Te_2P [Figs. 2(c)–(e)]. The spin-integrated ARPES results on both compounds, panels (a),(b),(d), reproduce the main experimental features discussed before. Our goal is to establish the spin texture of the Dirac-like dispersion along $\overline{\mathrm{KMK}}$ by measuring its in-plane spin component along the orthogonal $\overline{\Gamma M}$ direction. In the case of Ti_2Te_2P, the

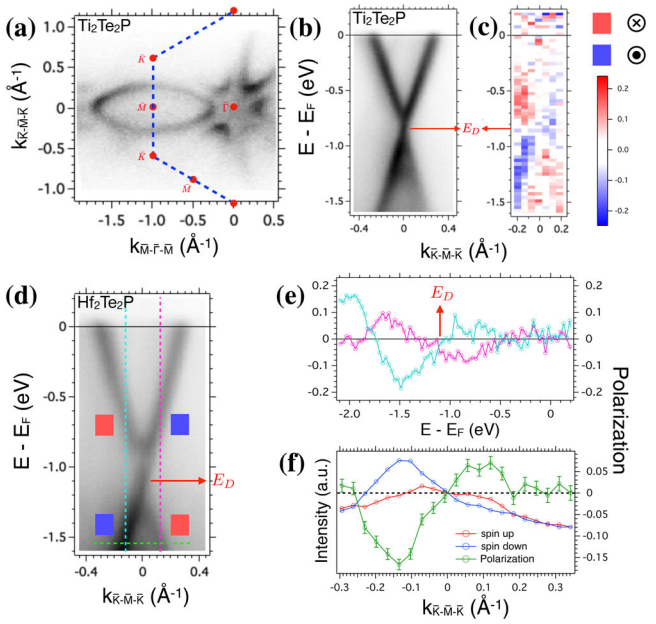

FIG. 2. (a) In-plane Fermi surface map of Ti_2Te_2P showing a sixfold symmetry. (b),(c) Near-E_F band structure of Ti_2Te_2P along the $\overline{KMK}$ high-symmetry line with spin-integrated, (b), and spin-resolved, (c), ARPES, showing a Dirac-like dispersion with clear spin polarization. The color scale in (c) represents the sign and value of the in-plane spin polarization along $\overline{\Gamma M}$ with blue (red) pointing toward (away from) the reader. (d) Near-E_F band structure of Hf_2Te_2P along the $\overline{KMK}$ high-symmetry line. Blue (red) squares indicate branches of the Dirac cone with spin polarization pointing toward (away from) the reader. (e) Energy dependent spin polarization of Hf_2Te_2P at the constant momenta indicated by the vertical light blue and magenta dashed lines in (c). (f) Spin-resolved momentum distribution curves (blue, red) and momentum dependent spin polarization (green) at the constant energy indicated by the horizontal green dashed line in (d). Spin up and spin down means parallel and antiparallel to $\overline{\Gamma M}$. The Dirac point at energy E_D is shown by a red arrow in panels (b)–(e). All data were collected with LH polarized photons of 55 eV. The temperature was 25 K.

energy-dependent spin polarization has been acquired at different k locations of the Dirac cone by measuring the spin-resolved energy distribution curves or EDCs (see the Supplemental Material [32]). Panel (c) is a stack of the energy-dependent polarization curves where the color scale represents the sign of the in-plane spin polarization with blue (red) pointing toward (away from) the reader. The Dirac-like dispersion is reproduced with a clear polarization reversal between the left and right sides of the cone. Moreover, our data reveal another reversal of the in-plane spin polarization between the top and bottom parts of the cone, in good agreement with results on Bi-based topological insulators [41].

Similar conclusions can be drawn on the in-plane spin polarization of Hf_2Te_2P, whose spin-integrated Dirac cone is shown in panel (d). The energy dependent spin polarization at both sides of the Dirac cone, shown in panel (e), has been acquired by means of spin-resolved EDCs. The polarization of each curve reverses above and below the Dirac point, while the two curves have opposite polarizations at a given binding energy. As expected, at the binding energy of the Dirac point (1.1 eV), the spin polarization is vanishingly small. Consistent information can be obtained with spin-resolved momentum distribution curves, shown in panel (f). Here the change in the direction of the in-plane spin polarization component is tracked as a function of momentum at a fixed binding energy at the bottom part of the Dirac cone (1.55 eV). At this binding energy, the polarization changes from negative to positive as one passes from the left to the right branch of the Dirac cone. This is in perfect agreement with the data shown in panel (e), where the light blue (magenta) curve obtained at the left (right) side of the cone shows a negative (positive) polarization at a binding energy of 1.55 eV. Based on the results presented in Fig. 2, we can experimentally confirm that the Dirac cone in compounds of the tetradymite family M_2Te_2X is spin-polarized.

Having established the spin polarization of the Dirac cone at $\bar{M}$, we now turn our attention to the characteristics and the spin texture of the linear features observed in the constant energy maps of Fig. 1. Figures 3(a), (b) show once more how the petal contours of the Fermi surface of Ti_2Te_2P evolve into linear features at the binding energy of the Dirac point. Panel (c) presents another measurement of the constant energy contours at the Dirac point energy, acquired with the experimental setup at HiSOR right before spin-resolved measurements. Figures 3(d)–(f) present the spin-resolved EDCs and the resulting energy-dependent spin polarization acquired at the left side of the Dirac cones, panels (g)–(i), themselves observed along three different k paths parallel to $\overline{KMK}$: cuts (1)–(3) in panel (c). These data show that an in-plane spin-polarization exists not only along the $\overline{KMK}$ high-symmetry direction but also all along the Dirac node arc. We conclude that the Dirac cones along $\overline{K\Gamma K}$ not only share a common energy for their Dirac point, forming the node arc, but also that they exhibit an identical spin polarization. Our experimental results can therefore establish that the observed linear features at the Dirac point energy correspond indeed to topologically nontrivial Dirac node arcs.

The aforementioned results confirm the presence of spin-polarized electrons with a Dirac-like dispersion in one direction and a very large effective mass in the perpendicular direction (see also Fig. S3 in the Supplemental Material [32]). Such qualitatively different behaviors may stem from the mixed contributions of p (≈60%–70%) and d (≈20%–30%) orbital states to the topological surface state at $\bar{M}$ (see Figs. S6 and S7 in the Supplemental Material [32]), as suggested for Ru_2Sn_3 [42]. Provided that the Dirac cone could be tuned near E_F, compounds of this family could give rise to highly

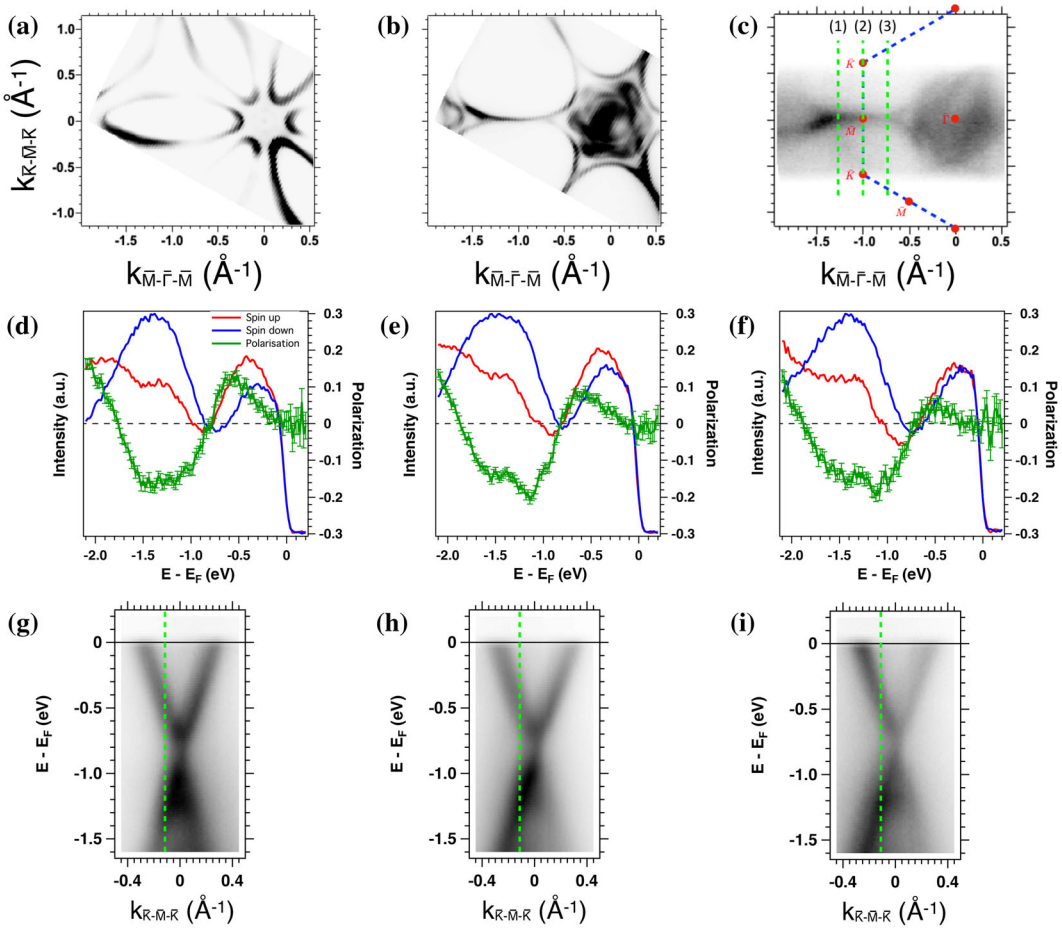

FIG. 3. (a),(b) Spin-integrated ARPES results obtained at synchrotron SOLEIL with LH polarized photons of 50 eV at a temperature of 6 K showing the Fermi surface contours of Ti_2Te_2P (a) and the existence of linear features at a binding energy of 0.85 eV (b). (c) Same as panel (b) but measured with LH photons of 55 eV at the ESPRESSO spin-resolved ARPES setup of beamline 9B at HiSOR. Path (1) corresponds to data shown in panels (d) and (g), path (2) to panels (e) and (f), and path (3) to panels (f) and (i). (d)–(f) Spin-resolved EDCs (red, blue) and energy dependent in-plane spin polarization parallel to $\overline{\Gamma M}$ (green) measured at the left branch of the Dirac cones [panels (g)–(i)], themselves obtained at different k locations along the Dirac node arc. (g)–(i) Energy-momentum dispersion along the k paths indicated in panel (c), with overlaid vertical dashed lines showing the k locations of the spin-resolved EDCs shown in panels (d)–(f). Panels (c)–(f) were all measured with LH photons of 55 eV at a temperature of 25 K.

anisotropic 2D electron systems with spin-polarized carriers. Our results prove that the existence of the Dirac node arcs is an inherent property of *all* studied M_2Te_2X compounds regardless of their topological character at $\bar{M}$, rather than being related to the weak topological character and the weak interlayer coupling of Hf_2Te_2P as suggested in Ref. [29]. After all, the Dirac states at $\bar{M}$ have a strong topological character for Zr_2Te_2P, Zr_2Te_2As, and Ti_2Te_2P [27,28].

The experimental observation of an in-plane spin polarization of the Dirac node arcs in a direction normal to the arcs' crystal momentum (i.e., parallel to $\overline{\Gamma M}$) agrees with the main direction of the spin-polarized vector in topological insulators and Rashba compounds [41,43]. The Supplemental Material [32] shows additional data for the out-of-plane spin polarization and discusses the magnitude of the observed spin polarization.

Surprisingly, there is substantial spin polarization at energies $E–E_F < -1.5$ eV, i.e., below the lower branch of the Dirac cone (Figs. 2 and 3). This observation has been reproduced in different experimental runs for all cleaved surfaces of both compounds studied here (Hf_2Te_2P and Ti_2Te_2P). On the other hand, it is not observed for compounds that do not belong to the M_2Te_2X family that were studied with the same setup. Therefore, we believe that it is not due to an experimental artifact, and it may indeed reveal the existence of spin-polarized states at larger binding energies. This scenario is in agreement with the experimental observation (e.g., Fig. 1) and the theoretical prediction [28] of holelike surface states at the same energy range. A possible explanation is the spin-polarized surface-confined states due to the Rashba-Bychkov effect, which have been repeatedly observed in the band structure of

Bi_2Se_3, in the vicinity of both the upper and the lower branches of its Dirac cone [44,45].

In conclusion, by means of spin-integrated and spin-resolved ARPES, we unambiguously proved the existence of type-I *topological* Dirac node arcs in compounds of the M_2Te_2X family. Our data showed bands with linear dispersion in one direction and a very large effective mass in the perpendicular direction. Our direct measurement of their spin-polarization vector shows substantial in-plane spin polarization in the direction perpendicular to the crystal momentum of the Dirac node arcs all along the linear features in the constant energy contours. This helical arrangement of the electron spins is opposite for the upper and lower branches of the Dirac cone forming the arc. Taken together, these observations establish the existence of topological Dirac node arcs in all studied compounds of the M_2Te_2X family regardless of their different topological characters. An exciting prospect for future research would be to tune, by doping or pressure, the energy of the Dirac points in the M_2Te_2X family to the Fermi level.

We thank F. Bertran for assistance during the ARPES measurements at CASSIOPEE (Synchrotron SOLEIL). The ARPES work at I. S. M. O. was supported by public grants from the French National Research Agency (ANR), project Fermi-NESt No. ANR-16-CE92-0018. Experiments at HiSOR were performed under the approval of the Program Advisory Committee (proposals 16BG014 and 17BU010). R. B. acknowledges support from the National Science Foundation through NSF/DMR1904361. L. B. is supported by DOE-BES through Award No. DE-SC0002613.

*Corresponding author.
ji.dai@epfl.ch
†Corresponding author.
emmanouil.frantzeskakis@u-psud.fr
‡Corresponding author.
andres.santander-syro@u-psud.fr
§Present address: Institute of Physics and Lausanne Centre for Ultrafast Science (LACUS), École Polytechnique Fédérale de Lausanne, CH-1015 Lausanne, Switzerland.
‖Present address: Condensed Matter Physics and Materials Science Division, Brookhaven National Laboratory, Upton, New York 11973, USA.
¶Present address: Department of Physics, University of Michigan, Ann Arbor, Michigan, USA.

[1] C. L. Kane and E. J. Mele, Phys. Rev. Lett. **95**, 146802 (2005).
[2] M. König, S. Wiedmann, C. Brüne, A. Roth, H. Buhmann, L. W. Molenkamp, X.-L. Qi, and S.-C. Zhang, Science **318**, 766 (2007).
[3] M. Z. Hasan and C. L. Kane, Rev. Mod. Phys. **82**, 3045 (2010).
[4] L. Fu, C. L. Kane, and E. J. Mele, Phys. Rev. Lett. **98**, 106803 (2007).
[5] X.-L. Qi and S.-C. Zhang, Rev. Mod. Phys. **83**, 1057 (2011).
[6] L. Fu, Phys. Rev. Lett. **106**, 106802 (2011).
[7] A. A. Soluyanov, D. Gresch, Z. Wang, Q. Wu, M. Troyer, X. Dai, and B. A. Bernevig, Nature (London) **527**, 495 (2015).
[8] Z. K. Liu, B. Zhou, Y. Zhang, Z. J. Wang, H. M. Weng, D. Prabhakaran, S.-K. Mo, Z. X. Shen, Z. Fang, X. Dai *et al.*, Science **343**, 864 (2014).
[9] S.-Y. Xu, C. Liu, S. K. Kushwaha, R. Sankar, J. W. Krizan, I. Belopolski, M. Neupane, G. Bian, N. Alidoust, T.-R. Chang *et al.*, Science **347**, 294 (2015).
[10] S.-Y. Xu, I. Belopolski, N. Alidoust, M. Neupane, G. Bian, C. Zhang, R. Sankar, G. Chang, Z. Yuan, C.-C. Lee *et al.*, Science **349**, 613 (2015).
[11] A. Stern and N. H. Lindner, Science **339**, 1179 (2013).
[12] V. Lahtinen and J. K. Pachos, SciPost Phys. **3** (2017).
[13] D. Pesin and A. H. MacDonald, Nat. Mater. **11**, 409 (2012).
[14] N. H. D. Khang, Y. Ueda, and P. N. Hai, Nat. Mater. **17**, 808 (2018).
[15] Z. Yue, B. Cai, L. Wang, X. Wang, and M. Gu, Sci. Adv. **2**, e1501536 (2016).
[16] Y. Wu, L.-L. Wang, E. Mun, D. D. Johnson, D. Mou, L. Huang, Y. Lee, S. L. Bud'ko, P. C. Canfield, and A. Kaminski, Nat. Phys. **12**, 667 (2016).
[17] D. Takane, Z. Wang, S. Souma, K. Nakayama, C. X. Trang, T. Sato, T. Takahashi, and Y. Ando, Phys. Rev. B **94**, 121108 (R) (2016).
[18] I. Knez, R.-R. Du, and G. Sullivan, Phys. Rev. Lett. **107**, 136603 (2011).
[19] Y. Xia, D. Qian, D. Hsieh, L. Wray, A. Pal, H. Lin, A. Bansil, D. Grauer, Y. S. Hor, R. J. Cava *et al.*, Nat. Phys. **5**, 398 (2009).
[20] Y. L. Chen, J. G. Analytis, J.-H. Chu, Z. K. Liu, S.-K. Mo, X. L. Qi, H. J. Zhang, D. H. Lu, X. Dai, Z. Fang *et al.*, Science **325**, 178 (2009).
[21] R. Noguchi, T. Takahashi, K. Kuroda, M. Ochi, T. Shirasawa, M. Sakano, C. Bareille, M. Nakayama, M. D. Watson, K. Yaji *et al.*, Nature (London) **566**, 518 (2019).
[22] M. Neupane, S.-Y. Xu, R. Sankar, N. Alidoust, G. Bian, C. Liu, I. Belopolski, T.-R. Chang, H.-T. Jeng, H. Lin *et al.*, Nat. Commun. **5**, 3786 (2014).
[23] A. A. Burkov, M. D. Hook, and L. Balents, Phys. Rev. B **84**, 235126 (2011).
[24] G. Bian, T.-R. Chang, R. Sankar, S.-Y. Xu, H. Zheng, T. Neupert, C.-K. Chiu, S.-M. Huang, G. Chang, I. Belopolski *et al.*, Nat. Commun. **7**, 10556 (2016).
[25] L. M. Schoop, M. N. Ali, C. Strasser, A. Topp, A. Varykhalov, D. Marchenko, V. Duppel, S. S. P. Parkin, B. V. Lotsch, and C. R. Ast, Nat. Commun. **7**, 11696 (2016).
[26] K.-W. Chen, S. Das, D. Rhodes, S. Memaran, T. Besara, T. Siegrist, E. Manousakis, L. Balicas, and R. E. Baumbach, J. Phys. Condens. Matter **28**, 14LT01 (2016).
[27] H. Ji, I. Pletikosić, Q. D. Gibson, G. Sahasrabudhe, T. Valla, and R. J. Cava, Phys. Rev. B **93**, 045315 (2016).
[28] K.-W. Chen, N. Aryal, J. Dai, D. Graf, S. Zhang, S. Das, P. Le Fèvre, F. Bertran, R. Yukawa, K. Horiba *et al.*, Phys. Rev. B **97**, 165112 (2018).
[29] M. M. Hosen, K. Dimitri, A. K. Nandy, A. Aperis, R. Sankar, G. Dhakal, P. Maldonado, F. Kabir, C. Sims, F. Chou *et al.*, Nat. Commun. **9**, 3002 (2018).
[30] C. Chen, X. Xu, J. Jiang, S.-C. Wu, Y. P. Qi, L. X. Yang, M. X. Wang, Y. Sun, N. B. M. Schröter, H. F. Yang *et al.*, Phys. Rev. B **95**, 125126 (2017).

[31] T. Okuda, K. Miyamaoto, H. Miyahara, K. Kuroda, A. Kimura, H. Namatame, and M. Taniguchi, Rev. Sci. Instrum. **82**, 103302 (2011).

[32] See Supplemental Material, which includes Refs. [33–40], at http://link.aps.org/supplemental/10.1103/PhysRevLett.126.196407 for technical details about the sample growth, crystal structure, and the ARPES and Spin-ARPES measurements.

[33] T. Okuda, Y. Takeichi, Y. Maeda, A. Harasawa, I. Matsuda, T. Kinoshita, and A. Kakizaki, Rev. Sci. Instrum. **79**, 123117 (2008).

[34] D. Hsieh, L. Wray, D. Qian, Y. Xia, J. H. Dil, F. Meier, L. Patthey, J. Osterwalder, G. Bihlmayer, Y. S. Hor *et al.*, New J. Phys. **12**, 125001 (2010).

[35] A. Takayama, T. Sato, S. Souma, and T. Takahashi, New J. Phys. **16**, 055004 (2014).

[36] T. Hirahara, K. Miyamoto, I. Matsuda, T. Kadono, A. Kimura, T. Nagao, G. Bihlmayer, E. V. Chulkov, S. Qiao, K. Shimada *et al.*, Phys. Rev. B **76**, 153305 (2007).

[37] F. Meier, H. Dil, J. Lobo-Checa, L. Patthey, and J. Osterwalder, Phys. Rev. B **77**, 165431 (2008).

[38] K. Yaji, Y. Ohtsubo, S. Hatta, H. Okuyama, K. Miyamoto, T. Okuda, A. Kimura, H. Namatame, M. Taniguchi, and T. Aruga, Nat. Commun. **1**, 17 (2010).

[39] C. Jozwiak, Y. L. Chen, A. V. Fedorov, J. G. Analytis, C. R. Rotundu, A. K. Schmid, J. D. Denlinger, Y.-D. Chuang, D.-H. Lee, I. R. Fisher, R J. Birgeneau, Z.-X. Shen, Z. Hussain, and A. Lanzara, Phys. Rev. B **84**, 165113 (2011).

[40] C. Jozwiak, C.-H. Park, K. Gotlieb, C. Hwang, D.-H. Lee, S. G. Louie, J. D. Denlinger, C. R. Rotundu, R. J. Birgeneau, Z. Hussain *et al.*, Nat. Phys. **9**, 293 (2013).

[41] D. Hsieh, Y. Xia, D. Qian, L. Wray, J. H. Dil, F. Meier, J. Osterwalder, L. Patthey, J. G. Checkelsky, N. P. Ong *et al.*, Nature (London) **460**, 1101 (2009).

[42] Q. D. Gibson, D. Evtushinsky, A. Yaresko, V. B. Zabolotnyy, M. N. Ali, M. K. Fuccillo, J. Van den Brink, B. Büchner, R. J. Cava, and S. V. Borisenko, Sci. Rep. **4**, 5168 (2014).

[43] J. Sánchez-Barriga, A. Varykhalov, J. Braun, S.-Y. Xu, N. Alidoust, O. Kornilov, J. Minár, K. Hummer, G. Springholz, G. Bauer *et al.*, Phys. Rev. X **4**, 011046 (2014).

[44] P. D. C. King, R. C. Hatch, M. Bianchi, R. Ovsyannikov, C. Lupulescu, G. Landolt, B. Slomski, J. H. Dil, D. Guan, J. L. Mi *et al.*, Phys. Rev. Lett. **107**, 096802 (2011).

[45] M. S. Bahramy, P. D. C. King, A. de la Torre, J. Chang, M. Shi, L. Patthey, G. Balakrishnan, P. Hofmann, R. Arita, N. Nagaosa *et al.*, Nat. Commun. **3**, 1159 (2012).